Supporting Information

Realization of SOMO-HOMO Level Conversion for a TEMPO-Dithiolate Ligand by Coodination to Platinum(II)

Tetsuro Kusamoto, Shoko Kume, and Hiroshi Nishihara*

Synthesis

(1) **2**

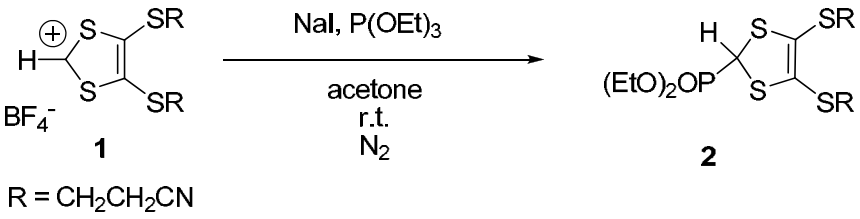

To an acetone solution (55 ml) of **1**[1] (0.685 g, 1.90 mmol), NaI (0.570 g, 3.80 mmol) and $P(OEt)_3$ (0.68 ml, 3.97 mmol) were added and stirred overnight at r.t.. The solvent was removed under a reduced pressure, and the residue was dissolved in CH_2Cl_2, and washed with water. The organic layer was dried, and the solvent was removed under a reduced pressure. The resulting solid was purified by silica gel column chromatography (eluent: CH_2Cl_2-AcOEt). **2** was obtained in 70% yield. Anal. Calcd for $C_{13}H_{19}N_2O_3PS_4$: C, 38.03; H, 4.68; N, 6.82. Found: C, 37.85; H, 4.61; N, 6.61. ^{1}H NMR ($CDCl_3$ 500 MHz): δ 1.39 (t, 6H, J = 7.1 Hz), 2.89 (m, 4H), 3.10 (m, 2H), 3.33 (m, 2H), 4.25 (m, 4H), 8.86 (d, 1H, J = 7.1 Hz).

(2) tempodt (chxdt)

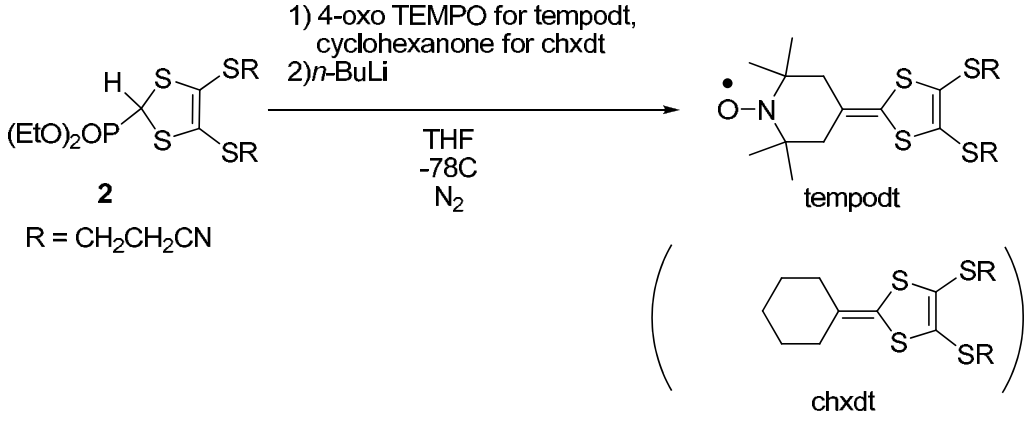

A solution of **2** (0.551g 1.32 mmol) and 1.3 eq. of corresponding ketone (4-oxo-TEMPO for tempodt, and cyclohexanone for chxdt) in dry THF at -78°C was added 1.1 equ. of n-BuLi (1.65 M, hexane sol.). After the filtration through alumina, solvent was removed under a reduced pressure. Resulting precipitate was purified by column chromatography (alumina, CH_2Cl_2-hexane as eluent for tempodt, silica gel, CH_2Cl_2 as eluent for chxdt). Recrystallization from CH_2Cl_2-hexane afforded yellow crystals (yield: 45% for tempodt, and 64% for chxdt).

tempodt: Anal. Calcd for $C_{18}H_{24}N_3OS_4$: C, 50.67; H, 5.67; N, 9.85. Found: C, 50.53; H, 5.65; N, 9.66.
chxdt: Anal. Calcd for $C_{15}H_{18}N_2S_4$: C, 50.81; H, 5.12; N, 7.90. Found: C, 50.65; H, 5.11; N, 7.79. ^{1}H NMR ($CDCl_3$ 500 MHz): δ 1.54 (br, 6H), 2.06 (t, 4H, J = 6.0 Hz), 2.75 (t, 4H, J = 7.1 Hz), 3.05 (t, 4H, J = 7.1 Hz).

(3) (tempodt)Pt

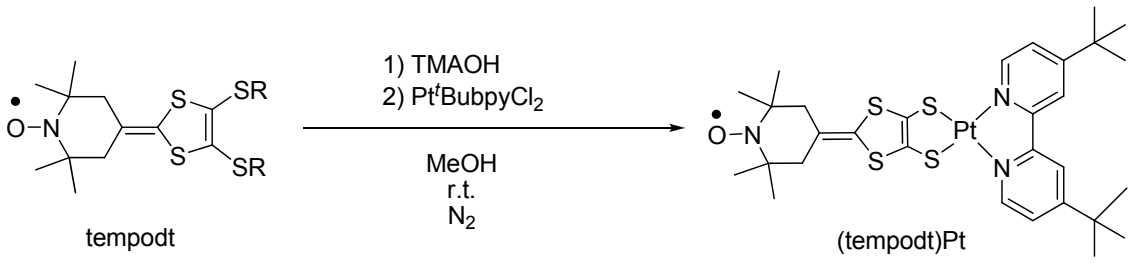

To a suspension of tempodt (52.2 mg, 0.122 mmol) in 15 ml of dry MeOH was added 4 eq. of TMAOH. The resulting suspension was stirred until tempodt was completely reacted, and Pt^{t}BubpyCl$_2$ (59.4mg, 0.111mmol) was added. The resulting precipitates were filtered, washed with MeOH and Et_2O, and dried in vacuo. Deep-blue solid was obtained by the recrystallization from CH_2Cl_2-hexane in 70%. Anal. Calcd for $C_{30}H_{40}N_3OPtS_4$: C, 46.08; H, 5.16; N, 5.37. Found: C, 45.84; H, 5.30; N, 5.09. MS (ESI-TOF+): *m/z* 781 $[M]^+$

(4) (chxdt)Pt

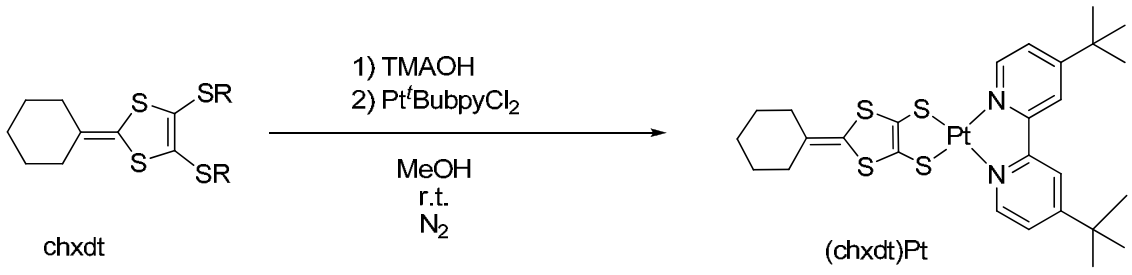

The synthetic method of (chxdt)Pt was the same as that of (tempodt)Pt except that chxdt was used instead of tempodt. Deep-blue microcrystals, yield: 76%. Anal. Calcd for $C_{27}H_{34}N_2PtS_4$: C, 45.51; H, 4.83; N, 3.95. Found: C, 45.68; H, 4.71; N, 3.68. MS (ESI-TOF+): *m/z* 709 $[M]^+$. ^{1}H NMR ($CDCl_3$ 500 MHz): δ 1.44 (s, 18H), 1.50 (s, 6.04H), 2.07 (br, 4H), 7.39 (d, 2H, J = 6.0 Hz), 7.89 (s, 2H), 8.86 (s, 2H, J = 6.0 Hz),

(5) $[(tempodt)Pt]_2(PF_6)_2$

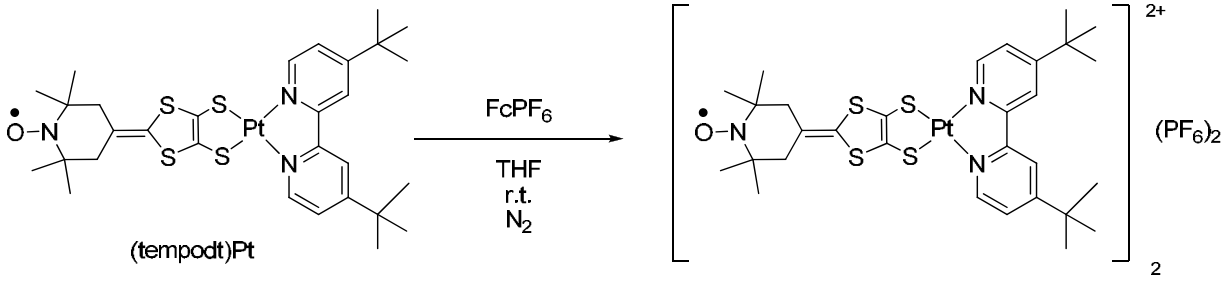

A solution of (tempodt)Pt (23.9 mg, 30.6 μmol) in degassed THF (5 ml) was added eq. of $FcPF_6$ (9.7 mg, 29.3 μmol) and stirred for 4 h at r.t.. Hexane was added to the solution, and resulting precipitates were filtered, washed with hexane and Et_2O, and dried under reduced pressure. Recrystallization from CH_2Cl_2-hexane gave deep green solid in 58% yield. Anal. Calcd for $C_{30}H_{40}N_3OPtS_4PF_6$: C, 38.92; H, 4.51; N, 4.25. Found: C, 38.87; H, 4.35; N, 4.53. MS (ESI-TOF+): *m/z* 781 $[(tempodt)Pt]^+$

(6) $[(chxdt)Pt]_2(PF_6)_2$

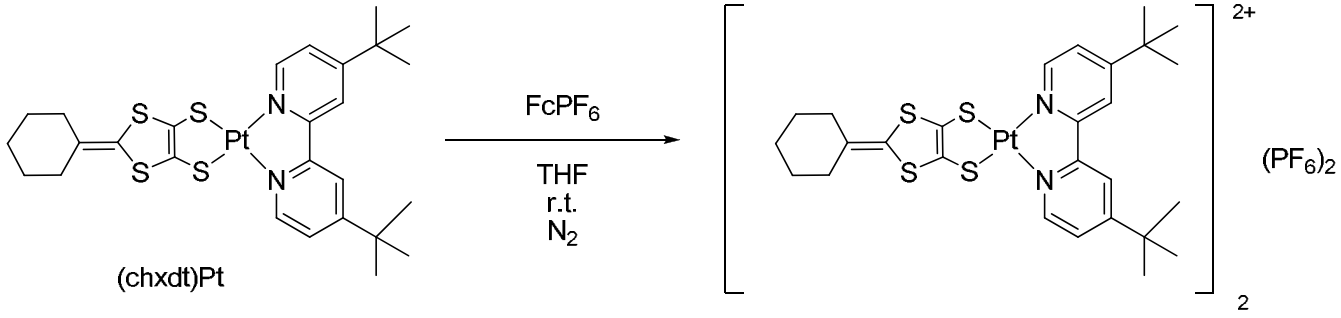

A solution of (chxdt)Pt (10.4 mg, 14.6 μmol) in degassed THF was added $FcPF_6$ (4.9 mg, 14.8 μmol) and stirred for 8 hours at r.t.. Hexane was added to the solution, and resulting precipitates were filtered, washed with hexane and Et_2O, and dried under reduced pressure. Deep purple solid was obtained in 73% yield. Anal. Calcd for $C_{27}H_{34}N_2PtS_4PF_6$: C, 37.93; H, 4.01; N, 3.28. Found: C, 38.15; H, 4.14; N, 3.04., MS (ESI-TOF+): *m/z* 708 $[(chxdt)Pt\text{-}H]^+$,1417 $[[(chxdt)Pt]_2\text{-}H]^+$.

References

1. Binet, L.; Fabre, J. M.; Montginoul, C.; Baek, S.; Becher, J. *J. Chem. Soc., Perkin Trans, 1*, **1996**, 783-788.

DFT calculations

Tempodt and chxdt: The geometry of tempodt and chxdt was fully optimized with the DFT (density functional theory) method with R = Me. The three-parametrized Becke-Lee-Yang-Parr (B3LYP) hybrid exchange-correlation functional was employed. The 6-31G(d) basis set was used for all atoms. Based on the optimized structure, TD-DFT (time-dependent density functional theory) method was performed to calculate excited states related to the absorption spectra of each compound. Solvent effect (CH_2Cl_2) was considered with PCM model. The present calculations were implemented with the Gaussian03 program package[1].

(tempodt)Pt and (chxdt)Pt: All the calculations were carried out with the functional of uMPW1PW91 for (tempodt)Pt and MPW1PW91 for (chxdt)Pt. The 6-31G(d) basis set was used for C, H, N,S, and O, and LanL2DZ(Hay-Wadt ECP) basis set was used for Pt atom,. Based on the optimized structure, TD-DFT (time-dependent density functional theory) method was performed to calculate excited states related to the absorption spectra of each compound. Solvent effect (CH_2Cl_2) was considered with PCM model. The present calculations were implemented with the Gaussian03 program package[1].

1. Frisch, M. J.; Trucks, G. W.; Schlegel, H. B.; Scuseria, G. E.; Robb, M. A.; Cheeseman, J. R.; Montgomery, Jr., J. A.; Vreven, T.; Kudin, K. N.; Burant, J. C.; Millam, J. M.; Iyengar, S. S.; Tomasi, J.; Barone, V.; Mennucci, B.; Cossi, M.; Scalmani, G.; Rega, N.; Petersson, G. A.; Nakatsuji, H.; Hada, M.; Ehara, M.; Toyota, K.; Fukuda, R.; Hasegawa, J.; Ishida, M.; Nakajima, T.; Honda, Y.; Kitao, O.; Nakai, H.; Klene, M.; Li, X.; Knox, J. E.; Hratchian, H. P.; Cross, J. B.; Adamo, C.; Jaramillo, J.; Gomperts, R.; Stratmann, R. E.; Yazyev, O.; Austin, A. J.; Cammi, R.; Pomelli, C.; Ochterski, J. W.; Ayala, P. Y.; Morokuma, K.; Voth, G. A.; Salvador, P.; Dannenberg, J. J.; Zakrzewski, V. G.; Dapprich, S.; Daniels, A. D.; Strain, M. C.; Farkas, O.; Malick, D. K.; Rabuck, A. D.; Raghavachari, K.; Foresman, J. B.; Ortiz, J. V.; Cui, Q.; Baboul, A. G.; Clifford, S.; Cioslowski, J.; Stefanov, B. B.; Liu, G.; Liashenko, A.; Piskorz, P.; Komaromi, I.; Martin, R. L.; Fox, D. J.; Keith, T.; Al-Laham, M. A.; Peng, C. Y.; Nanayakkara, A.; Challacombe, M.; Gill, P. M. W.; Johnson, B.; Chen, W.; Wong, M. W.; Gonzalez, C.; Pople, J. A. *Gaussian03, Revision C.02*, Gaussian, Inc., Pittsburgh PA, **2003**.

Table S1. The potentials (V vs Fc/Fc^{+}) at the first reduction $E^{1st\ red}$ and anodic peak maximum of the first oxidation $E_p^{1st\ ox.}$ of each compound obtained by CV measurements.

compound	$E_p^{1st\ ox.}$ / V	$E^{1st\ red.}$ / V
tempodt	0.22	-
chxdt	0.36	-
TEMPO	0.36	-
(tempodt)Pt	-0.26	-1.80
(chxdt)Pt	-0.24	-1.79

Table S2. Absorption wavelength and ε of each compound. The corresponding transition energies and oscillator strengths calculated by TD-DFT method are also shown.

compound	λ_{max}[a] / nm	ε_{max} / $M^{-1}cm^{-1}$	E_{max}[a] /eV	E_{calc}[b] /eV	f[c] / osillator strength
tempodt	369	2055	3.36	3.30	0.0068
	335	3220	3.69	3.59	0.0596
	260	11770	4.77	4.88	0.3550
chxdt	367	2470	3.38	3.51	0.0649
	339	2970	3.65	3.66	0.0128
	260	11200	4.77	4.94	0.1916
				4.99	0.1475
(tempodt)Pt	645	4199	1.92	1.79	0.1146
	391	3300	3.17	3.06	0.0759
(chxdt)Pt	654	3933	1.90	1.74	0.1104
	400	3390	3.10	2.96	0.0798

a Absorption maxima

b Corresponding transition energy calculated by TD-DFT method

c Osillator strength calculated by TD-DFT method

Table S3. Crystal data and refinement parameters for tempodt and (tempodt)Pt.

	tempodt	**(tempodt)Pt**
Empirical formula	$C_{18}H_{24}N_3OS_4$	$C_{30}H_{40}N_2OPtS_4$
Fw	426.68	781.98
Crystal dimension	0.30 ×0.10 × 0.05 mm	0.10 ×0.03 × 0.03 mm
Crystal system	Monoclinic	Orthorhombic
Lattice parameters	*a* = 18.214(6)	a = 19.30(2)
	b = 12.083(4)	b = 22.99(2)
	c = 9.586(3)	c = 7.060(6)
	β = 101.953(1)	
	V = 2064.0(1)	*V* = 3132(5)
Space group	$P2_1/c$	*Cmc*21
Z value	4	4
λ	0.7107 Å	0.7107 Å
T	93 K	93 K
μ(Mo Kα)	0.473 mm^{-1}	4.775 mm^{-1}
D(calc)	1.373 g/cm^3	1.658 g/cm^3
R_1	0.0452	0.0898
WR_2	0.0952	0.2442
GOF	1.085	1.037

[a] $R_1 = \Sigma||F_o| - |F_c||/\Sigma|F_o|$ ($I > 2\sigma(I)$).

[b] $wR_2 = [\Sigma(w(F_o^2 - F_c^2)^2)/\Sigma w(F_o^2)^2]^{1/2}$ ($I > 2\sigma(I)$).

[c] $GOF = [\Sigma(w(F_o^2 - F_c^2)^2)/\Sigma(N_0\text{-}N\nu)^2]^{1/2}$.

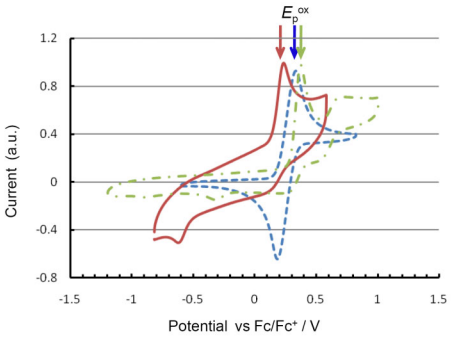

Figure S1. Cyclic voltammogram of tempodt (red, plain line), chxdt (green, dotted and dashed line) and TEMPO (blue, dashed line) at 100 $mV \cdot s^{-1}$ in 0.1 M Bu_4NClO_4-CH_2Cl_2 at 298 K. Arrows show the peaks of each oxidation peak potential (E_p^{ox}).

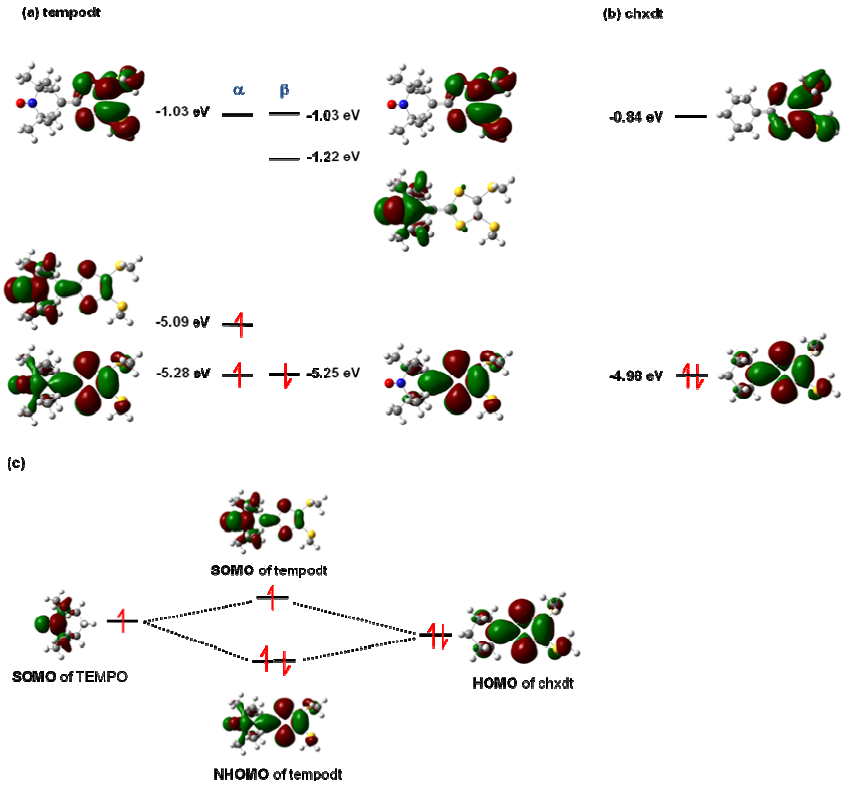

Figure S2. Calculated orbitals and energies of tempodt (a) and chxdt (b) and schematic representation of the interaction of each orbital for tempodt (α orbital is shown in NHOMO) (c).

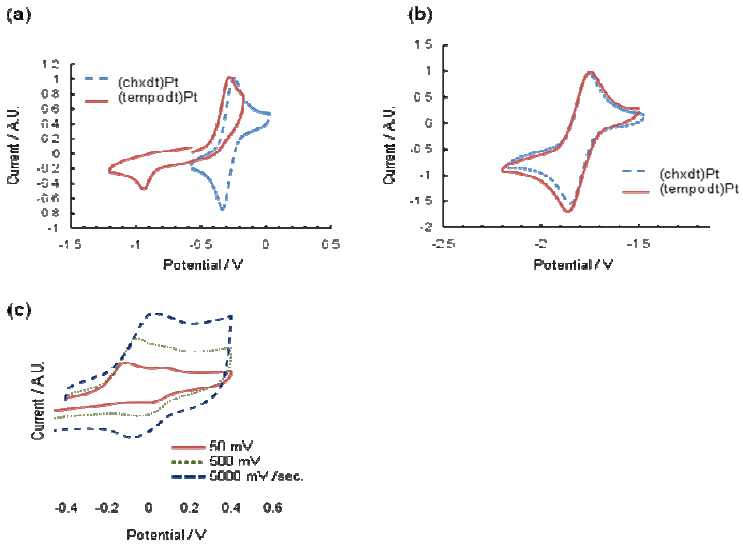

Figure S3. Cyclic voltammograms of (tempodt)Pt (red, plain line) and (chxdt)Pt (blue, dashed line). The potentials are given in V vs Fc/Fc^{+}. 1st oxidation region (a), 1st reduction region (b), and sweep rate dependence of the oxidation wave of (tempodt)Pt. dashed line: 5 V / s., dotted line: 500 mV / s, plain line: 50 mV / s (c). We note that the first oxidation of (tempodt)Pt is irreversible at a scan rate of 100 mV/s, but becomes quasi-reversible at higher scan rates. This result indicates that the following chemical reaction occurs after the oxidation. These results support the UV-Vis spectroscopic results. (for the spectroscopic results, see Figure S6)

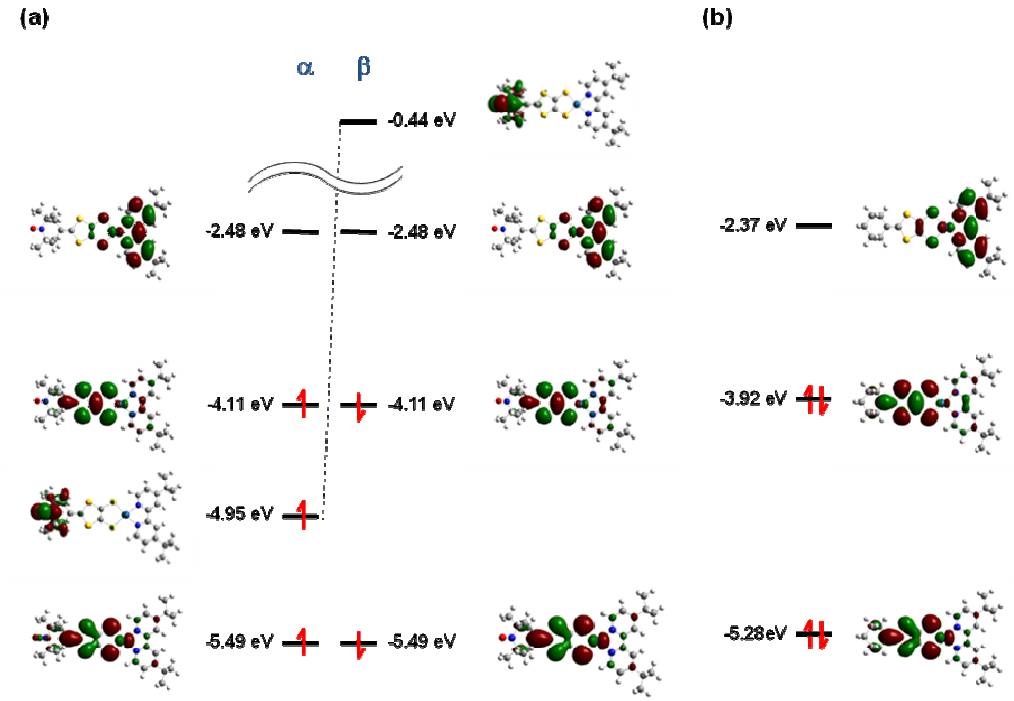

Figure S4. MOs and energy levels of (tempodt)Pt (a) and (chxdt)Pt (b).

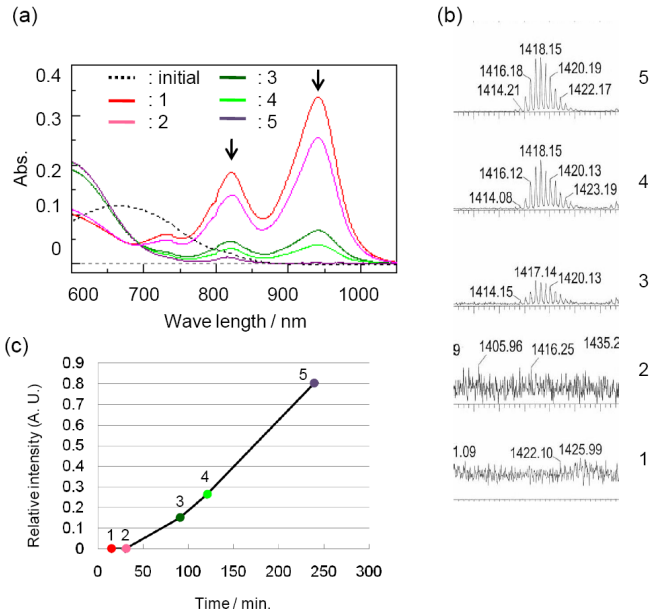

Figure S5. Observed VIS-NIR absorption spectra during the oxidation of (chxdt)Pt. initial: before oxidation (= (chxdt)Pt), 1: 15 min, 2: 30 min, 3: 90 min, 4: 120 min, 5. 240 min (= reaction completed), after the addition of $[Fe(C_5H_5)_2]PF_6$ in CH_2Cl_2 at r.t.. UV-Vis spectra (a), Observed ESI-TOF Mass spectra around 1419 (1419.82 is the calculated molecular weight of $[(chxdt)Pt)_2]^+$) (b), and the temperature dependence of the relative intensity $I_{dimer}/I_{monomer}$ (Dimer species show main peaks around *m/z* = 709 $[(chxdt)Pt]^+$ and sub peaks at *m/z* = 1418 $[[(chxdt)Pt]_2]^+$, and the intensities are described as $I_{monomer}$ and I_{dimer}, respectively) (c).

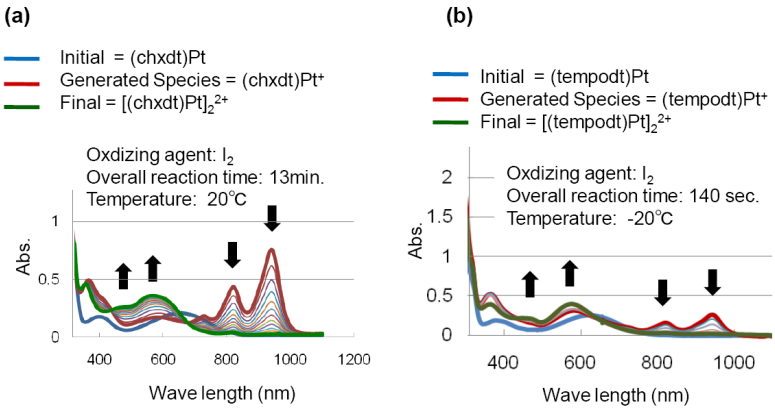

Figure S6. Changes in spectra during the oxidation of (chxdt)Pt (a) and (tempodt)Pt (b) in CH_2Cl_2. The reaction rate of (tempodt)Pt was much higher than that of (chxdt)Pt. These results correspond to their electrochemical behavior in which CV around the first oxidation of (tempodt)Pt showed sweep rate dependence (Figure S3(c)).

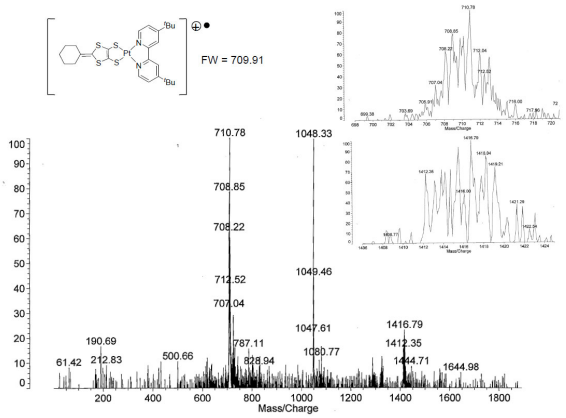

Figure S7. MALDI-TOF mass spectrum of $[(chxdt)Pt]_2(PF_6)_2$.

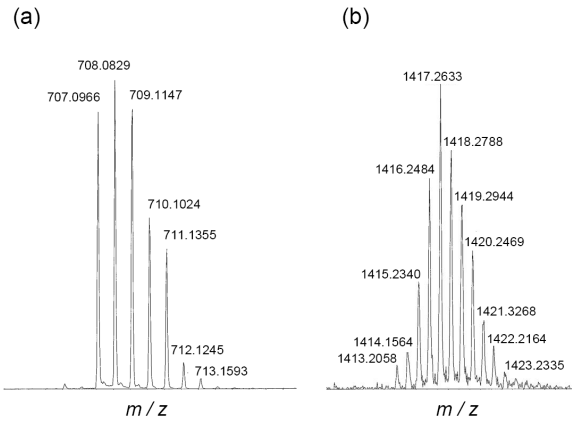

Figure S8. ESI-TOF mass spectra of $[(chxdt)Pt]_2(PF_6)_2$. Main peaks around *m/z*: 709 $[(chxdt)Pt]^+$ (a) and sub peaks around *m/z*: 1418 $[[(chxdt)Pt]_2]^+$ (b).

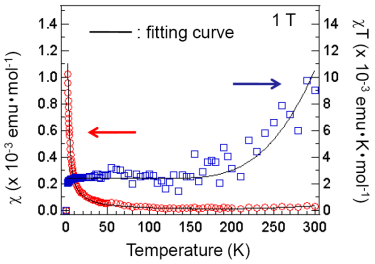

Figure S9. The temperature dependence of magnetic susceptibility χ and χT of $[(chxdt)Pt]_2(PF_6)_2$. Data are fitted according to the dimer model (J/k_b = -780 K) + curie law (0.6% of S = 1/2 spin, this corresponds to paramagnetic impurity)

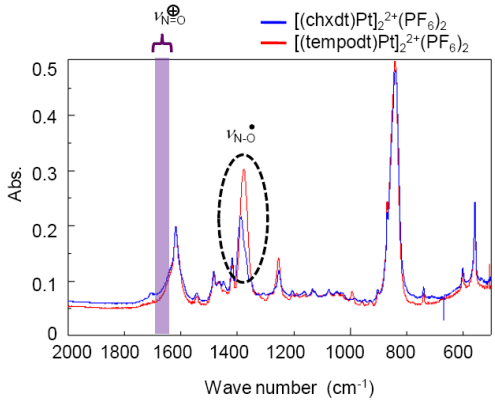

Figure S10. IR spectra of [(tempodt)Pt]$_2$(PF$_6$)$_2$ (= red) and [(chxdt)Pt]$_2$(PF$_6$)$_2$ (= blue). Dashed circle indicates the peak resulting from the N-O radical bond stretching mode. [(tempodt)Pt]$_2$(PF$_6$)$_2$ does not show any peak at around 1650 – 1700 cm^{-1} (shown in purple box, N=O$^+$ stretching mode is expected in this range), suggesting that N-O radical is not oxidized.

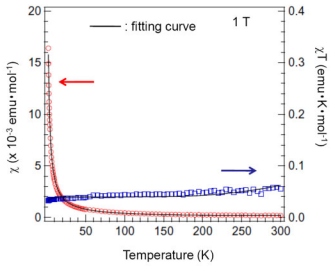

Figure S11. The temperature dependence of magnetic susceptibility χ and χT of $[(tempodt)Pt]_2(PF_6)_2$. Data are fitted according to the dimer model (J/k_b = -625 K, this part corresponds to the antiferromagnetically coupled π-radicals on HOMO) + Curie Weiss law (C = 0.040 emu·K·mol^{-1}, θ = -0.5 K, this is considered to the contribution from TEMPO moiety.)

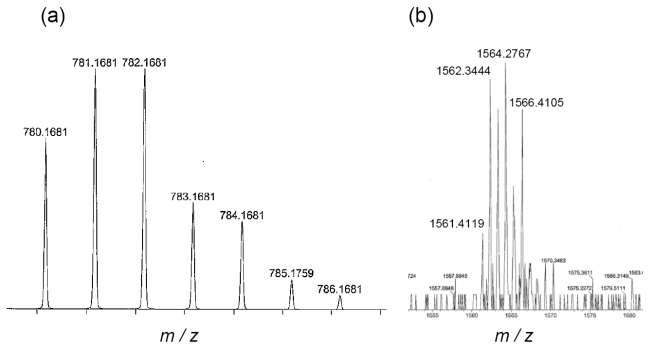

Figure S12. ESI-TOF mass spectrum of $[(tempodt)Pt]_2(PF_6)_2$. Main peaks around *m/z*: 781 $[(tempodt)Pt]^+$ (a) and sub peaks around *m/z*: 1562 $[[(tempodt)Pt]_2]^+$ (b).

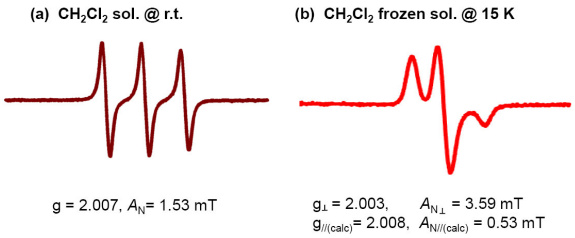

Figure S13. ESR spectra of $[(tempodt)Pt]_2(PF_6)_2$ in CH_2Cl_2 at r.t. (a) and at 15 K (frozen solution) (b). Obtained parameters are also given.